remote sensing

MDPI

Article

Comparative Sensitivity of Vegetation Indices Measured via Proximal and Aerial Sensors for Assessing N Status and Predicting Grain Yield in Rice Cropping Systems

Telha H. Rehman [1,*], Mark E. Lundy [1,2] and Bruce A. Linquist [1,2]

[1] Department of Plant Sciences, University of California, Davis, CA 95616, USA; melundy@ucdavis.edu (M.E.L.); balinquist@ucdavis.edu (B.A.L.)
[2] Division of Agriculture and Natural Resources, University of California, Davis, CA 95618, USA
* Correspondence: trehman@ucdavis.edu

Abstract: Reflectance-based vegetation indices can be valuable for assessing crop nitrogen (N) status and predicting grain yield. While proximal sensors have been widely studied in agriculture, there is increasing interest in utilizing aerial sensors. Given that few studies have compared aerial and proximal sensors, the objective of this study was to quantitatively compare the sensitivity of aerially sensed Normalized Difference Vegetation Index (NDVI) and Normalized Difference Red-Edge Index (NDRE) and proximally sensed NDVI for assessing total N uptake at panicle initiation (PI-N_{UP}) and predicting grain yield in rice. Nitrogen response trials were established over a 3-year period (10 site-years) at various locations throughout the Sacramento Valley rice growing region of California. At PI, a multispectral unmanned aircraft system (UAS) was used to measure $NDVI_{UAS}$ and $NDRE_{UAS}$ (average ground sampling distance: 3.7 cm $pixel^{-1}$), and a proximal GreenSeeker (GS) sensor was used to record $NDVI_{GS}$. To enable direct comparisons across the different indices on an equivalent numeric scale, each index was normalized by calculating the Sufficiency-Index (SI) relative to a non-N-limiting plot. Kernel density distributions indicated that $NDVI_{UAS}$ had a narrower range of values that were poorly differentiated compared to $NDVI_{GS}$ and $NDRE_{UAS}$. The critical PI-N_{UP} where yields did not increase with higher PI-N_{UP} averaged 109 kg N ha^{-1} ($\pm$4 kg N ha^{-1}). The relationship between SI and PI-N_{UP} for the $NDVI_{UAS}$ saturated lower than this critical PI-N_{UP} (96 kg N ha^{-1}), whereas $NDVI_{GS}$ and $NDRE_{UAS}$ saturated at 111 and 130 kg N ha^{-1}, respectively. This indicates that $NDVI_{UAS}$ was less suitable for making N management decisions at this crop stage than $NDVI_{GS}$ and $NDRE_{UAS}$. Linear mixed effects models were developed to evaluate how well each SI measured at PI was able to predict grain yield. The $NDVI_{UAS}$ was least sensitive to variation in yields as reflected by having the highest slope (2.4 Mg ha^{-1} per 0.1 SI). In contrast, the slopes for $NDVI_{GS}$ and $NDRE_{UAS}$ were 0.9 and 1.1 Mg ha^{-1} per 0.1 SI, respectively, indicating greater sensitivity to yields. Altogether, these results indicate that the ability of vegetation indices to inform crop management decisions depends on the index and the measurement platform used. Both $NDVI_{GS}$ and $NDRE_{UAS}$ produced measurements sensitive enough to inform N fertilizer management in this system, whereas $NDVI_{UAS}$ was more limited.

Keywords: rice; nitrogen; precision management; grain yield; panicle initiation; canopy reflectance; Sufficiency-Index; NDVI; NDRE; UAS; GreenSeeker

Citation: Rehman, T.H.; Lundy, M.E.; Linquist, B.A. Comparative Sensitivity of Vegetation Indices Measured via Proximal and Aerial Sensors for Assessing N Status and Predicting Grain Yield in Rice Cropping Systems. *Remote Sens.* **2022**, *14*, 2770. https://doi.org/10.3390/rs14122770

Academic Editor: Michael Schirrmann

Received: 6 May 2022
Accepted: 2 June 2022
Published: 9 June 2022

1. Introduction

Remote sensing has emerged as a powerful technology to inform sustainable agronomic management by providing an accurate and timely assessment of the status of developing crops [1]. Agricultural remote sensing is based on the collection of crop canopy reflectance spectra at specific wavelengths in the electromagnetic spectrum, usually corresponding to regions where the canopy experiences strong absorption or reflectance of

incoming radiation [2]. A common method to interpret canopy reflectance data is to use the wavelengths to develop a vegetation index (VI), which is a mathematical combination of wavelengths related to specific biophysical characteristics of the plant [3]. Over the past decade, sensors have developed rapidly with higher spatial and spectral resolution. Similarly, better platforms are available that can carry such sensors and easily maneuver over large areas, which has led to a significant broadening of remote sensing applications in many fields including agriculture [4]. Some of the current applications of remotely sensed data in agriculture include biomass estimation, assessing crop nutritional status, detecting plant stress, identifying disease incidence, scouting for weeds, and predicting potential yield.

Some important applications of remote sensing in rice (*Oryza sativa* L.) are the assessment of crop nitrogen (N) status and prediction of grain yield. Nitrogen is an essential element for plant growth, and an adequate supply of N is fundamental to maximizing rice grain yield and quality [5]. However, overapplication of N fertilizer in rice and other crops has been associated with reduced yields and lodging [6], as well as harmful impacts on the environment through nitrate leaching [7], greenhouse gas emissions [8], or eutrophication of downstream aquifers [9]. The most accurate method to assess plant N status is by plant tissue analysis, but this technique is time consuming and lab results are often received past the time when decisions need to be made [10]. Alternative methods to assess N status in rice include using the Soil Plant Analysis Development (SPAD) chlorophyll meter [11] or the Leaf Color Chart [12]. While these tools are useful, they are limited by their single leaf sampling method, thus making it difficult to utilize these tools to accurately assess crop N status over large areas [10,13]. The development of remote sensing techniques provides a promising alternative to address this issue.

Remote sensing data can be collected using different platforms, including proximal handheld sensors or aerial sensors mounted to airplanes, satellites, or unmanned aerial vehicles (UAV; sensor mounted to a UAV is referred to as an unmanned aircraft system, UAS) [4]. Over the past two decades, most agricultural remote sensing research has focused on the use of proximal sensors, especially those that utilize an active light source [13]. However, with the recent expansion of compact aerial sensors that can be easily mounted to a UAV, an increasing number of studies have shifted toward utilizing UAS-based platforms [14]. Relative to proximal and UAS-based remote sensing, airplane and satellite-based measurements are less frequently used in agricultural applications due to the high complexity and costs of operating an airplane and insufficient spatial and temporal resolution often experienced with satellite imagery [15]. However, despite being more convenient than airplane and satellite-based remote sensing, both proximal and UAS-based remote sensing also come with their own unique advantages and disadvantages.

Among proximal sensors, the GreenSeeker (GS) HandHeld (Trimble Inc., Sunnyvale, CA, USA) has been one of the most commonly used in agricultural research. It is an active canopy sensor, which permits the collection of reflectance data at any time of day, regardless of ambient light conditions or cloud cover [13]. The GS measures canopy reflectance at specific bands in the red (670 nm) and near infrared (780 nm) spectral regions and displays the Normalized Difference Vegetation Index (NDVI), which is a useful measure of plant productivity and is among the most commonly measured indices in agricultural remote sensing applications [16,17]. Studies have tested the utility of GS NDVI ($NDVI_{GS}$) as an N management tool in rice systems and reported strong correlations between $NDVI_{GS}$ and aboveground biomass, total N uptake (N_{UP}), and grain yields [18–20]. Others have reported similar results for wheat (*Triticum aestivum*) [21] and maize (*Zea mays*) [22,23]. However, despite showing good utility in these crops, a key disadvantage of the GS is that it only measures NDVI, which loses sensitivity (i.e., saturates) once crop biomass exceeds a certain threshold [17].

When collecting canopy reflectance data aerially, typically a passive multispectral sensor is mounted to a UAV and flown in a grid-style pattern over the field or experimental area. This facilitates the assessment of larger areas and enables the identification of spatial

variability that is often present within a field [24–26]. An example of one such multispectral sensor frequently used in agricultural applications is the MicaSense Red-Edge M (MicaSense, Inc., Seattle, WA, USA). This is a passive sensor that collects canopy reflectance across five spectral bands (blue, green, red, red-edge, and near infrared) [27]. The additional bands included in multispectral sensors such as the MicaSense sensor, provide an important advantage over proximal sensors like the GS in that they permit the calculation of a range of indices, including red-edge-based indices, among which the Normalized Difference Red-Edge Index (NDRE) is the most common [28]. The NDRE is based on a similar calculation to the NDVI, but incorporates a red-edge band in place of red, which allows the NDRE to be more resistant to the saturation problem inherent with NDVI [29,30]. Additionally, data collected with aerial multispectral sensors permit the use of more complex non-index-based classification techniques, such as spectral mixture models, texture analysis, or machine learning algorithms [31–33], which can also be used in combination with VIs to improve crop N status assessments by reducing saturation [34,35]. However, aerial-based remote sensing also has its own limitations, including the narrow timeframe around solar noon during which data are best collected, the high cost of UAS platforms, and the technical issues that UAS platforms can experience mid-air, such as loss of power or an engine breakdown [36,37].

Among studies that only used aerial sensors to assess N status in rice, Dunn et al. (2016) [28] reported strong correlations between NDVI and NDRE and N_{UP}, but found that NDRE saturated less than NDVI. Wang et al. (2021) [34] reported stronger correlations between NDRE and Red-Edge Chlorophyll Index when estimating N-index (ratio of N concentration between fertilized and non-fertilized plants), relative to NDVI, and Zheng et al. (2019) [38] reported that Red-Edge Chlorophyll Index correlated better with rice aboveground biomass than NDVI. In similar experiments on other crops, Walsh et al. (2018) [39] found that the red-edge-based indices exhibited a higher correlation with wheat N concentration than red-based indices. Becker et al. (2020) [40] did not evaluate NDVI but reported a stronger correlation between NDRE and grain yield than Green Leaf Index and Blue Reflectance Index in maize.

Although numerous studies have demonstrated the ability of NDVI and NDRE to assess crop N status and predict yields using either a proximal sensor or an aerial sensor, few studies have directly compared proximal and aerial sensors side-by-side. Among the few studies that have, Zheng et al. (2018) [41] reported that proximal NDVI (measured using a passive hyperspectral sensor) was better correlated with rice N concentration than aerial NDVI. Sumner et al. (2021) [42] measured NDVI and NDRE in maize and found that proximal NDVI and aerial NDRE were both more sensitive to changes in N fertilizer rate than aerial NDVI. In wheat, Hassan et al. (2018) [43] and Duan et al. (2017) [44] both found proximal and aerial NDVI measurements to be well-correlated to each other across a wide range of growth stages, though Duan et al. (2017) [44] reported that aerial NDVI measurements were confined to a narrower range than proximal NDVI.

Given the interest and promise of canopy reflectance technology along with the lack of studies comparing platforms and sensors, the objective of this study was to compare the sensitivity of aerially sensed NDVI and NDRE to proximally sensed NDVI for assessing N status and predicting grain yield of rice at panicle initiation (PI) growth stage. Specifically, the level at which each index saturated relative to total N uptake at PI (PI-N_{UP}) was quantified and examined relative to important thresholds for fertilizer N management in this system. Additionally, the relative sensitivity of each index to predict grain yield at PI was quantified as the slope of the resulting linear relationship. This was accomplished through field studies over a 3-year period at 10 locations throughout the Sacramento Valley rice growing region of California (CA), USA.

2. Materials and Methods

2.1. Site Description

Ten replicated N response trials (nine on-farm; one on-station) were established during the 2017 to 2019 rice growing seasons (referred to by proximity to nearest town or station and study year) throughout the Sacramento Valley rice growing region of CA (Figure 1, Table 1). The on-station site was established at the CA Rice Experiment Station (RES) near Biggs. The Sacramento Valley has a Mediterranean climate characterized by warm and dry conditions during the growing season (May to October). The average air temperature and precipitation during the three years of this study were 23.2 °C and 5.9 mm, respectively [45]. Pre-season soil samples were collected from the plow layer (approximately 0–15 cm) after tillage and prior to fertilizer application at each site and analyzed for pH, particle size, organic carbon, and total N. The soil properties at each site were typical for rice soils in this region (Table 1).

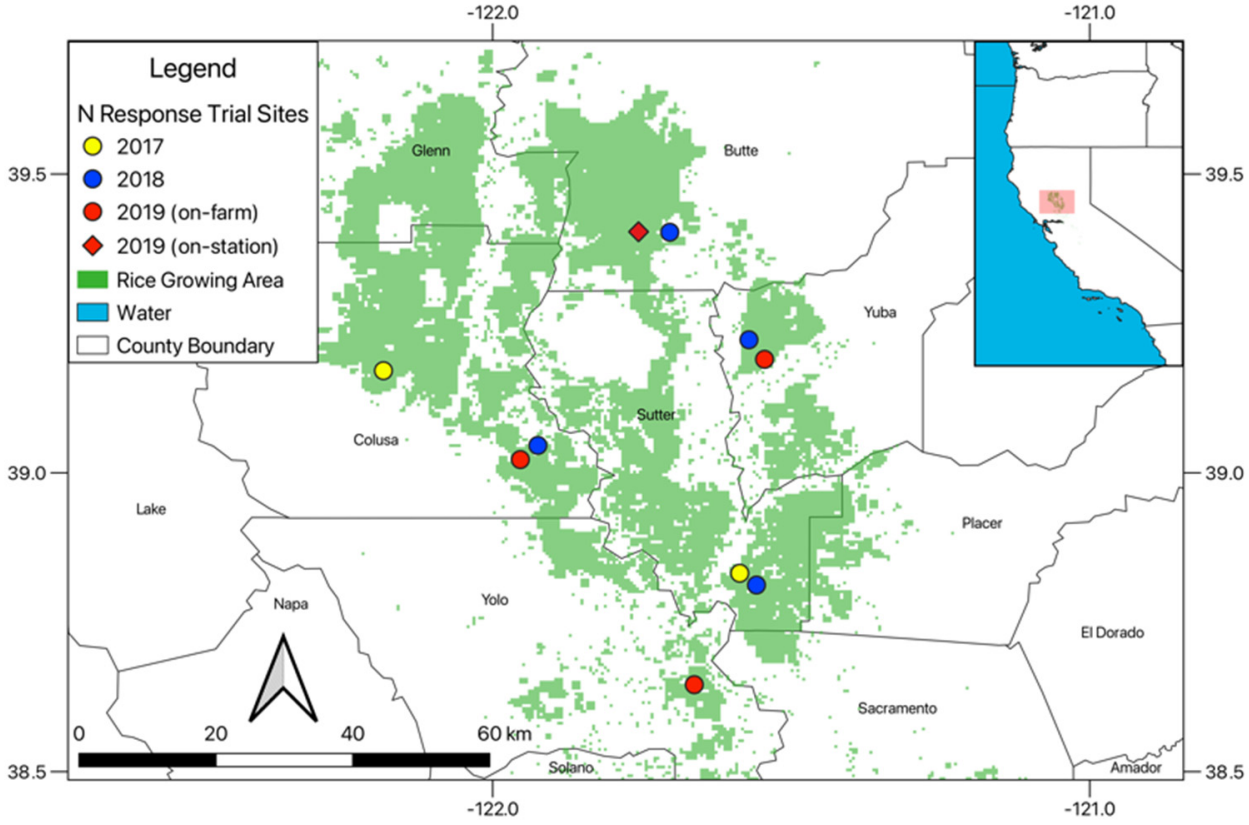

Figure 1. A map of N response trial sites established during the 2017 to 2019 growing seasons throughout the Sacramento Valley rice growing area of California, USA.

2.2. Experimental Design

Each N response trial was arranged as a randomized complete block design with four replicates. Treatments were pre-plant N fertilizer rates. In 2017, pre-plant N fertilizer was applied as urea at rates ranging from 0 to 225 kg N ha^{-1}, and in 2018 and 2019 pre-plant N fertilizer was applied as aqua-ammonia at rates ranging from 0 to 235 kg N ha^{-1}. Potassium (K) and phosphorus (P) fertilizers were broadcast across all plots at rates of 50 kg K_2O ha^{-1} as sulfate of potash and 45 kg P_2O_5 ha^{-1} as triple superphosphate to ensure these nutrients did not limit crop growth. The rice crop was established using water-seeding at all sites, which is the common practice in CA [46]. In this case, the fields are fertilized following seedbed preparation, flooded, and then soaked seed is broadcast onto the field by airplane. The medium grain rice variety M-206, which is commonly grown in CA, was planted at all sites. Herbicide and irrigation management followed common grower practice and was either managed by the growers (on-farm sites) or researchers (on-station site). The fields

remained continuously flooded until three weeks before harvest when they were drained to prepare for harvest.

Table 1. Soil descriptions and selected properties of each N response trial site-year located throughout the Sacramento Valley, California.

Site-Year	Soil Series	Taxonomic Classification	Texture (%)			Organic Carbon (%)	Total Nitrogen (%)	pH
			Sand	Silt	Clay			
Nicolaus-17	Capay	Fine, smectitic, thermic Typic Haploxererts	19	36	45	1.51	0.12	5.5
Williams-17	Willows	Fine, smectitic, thermic Sodic Endoaquerts	21	39	40	1.75	0.15	5.0
Arbuckle-18	Clear Lake	Fine, smectitic, thermic Xeric Endoaquerts	30	21	49	1.95	0.16	6.3
Biggs-18	Eastbiggs	Fine, mixed, active, thermic Abruptic Durixeralfs	50	30	20	1.60	0.12	4.9
Marysville-18	San Joaquin	Fine, mixed, active, thermic Abruptic Durixeralfs	39	39	22	1.64	0.13	4.6
Nicolaus-18	Capay	Fine, smectitic, thermic Typic Haploxererts	22	36	42	1.67	0.14	4.8
Arbuckle-19	Clear Lake	Fine, smectitic, thermic Xeric Endoaquerts	8	38	55	1.99	0.16	6.3
Davis-19	Sycamore	Fine-silty, mixed, super active, nonacid, thermic Mollic Endoaquepts	9	38	53	1.98	0.18	6.3
Marysville-19	San Joaquin	Fine, mixed, active, thermic Abruptic Durixeralfs	35	41	24	1.54	0.12	4.7
RES-19	Esquon-Neerdobe	Fine, smectitic, thermic Xeric Epiaquerts	30	26	44	1.38	0.11	5.3

2.3. Plant Sampling and Analysis

Biomass was collected at PI after canopy reflectance measurements (see below) by pulling all rice plants within a 0.5 m^2 quadrat from every plot. Within 24 h of collecting the samples, the biomass was washed to remove any residual soil, the roots were removed, and the aboveground shoots were oven dried to constant weight at 60 °C. Samples were then ground to pass a 4-mm sieve and ball-milled. Plant material was analyzed for total N using an elemental analyzer interfaced to a continuous flow isotope ratio mass spectrometer (EA-IRMS) [47]. From these samples, PI-N_{UP} was quantified as the product of aboveground biomass and N concentration. Rehman et al. (2019) [19] previously reported that $NDVI_{GS}$ best assessed PI rice N status when quantified as PI-N_{UP}, rather than plant N concentration or aboveground biomass. Thus, PI-N_{UP} was selected as the N status parameter for the basis of comparison across the indices in this study.

Grain yield was determined at physiological maturity by harvesting all plants from a 1.0 m^2 quadrat. Grains were removed from panicles, cleaned using a seed blower, dried to constant moisture at 60 °C, and then weighed. Grain yields are reported at 14% moisture.

2.4. Measuring Canopy Reflectance

2.4.1. Sensors Used for Measuring NDVI and NDRE

The NDVI and NDRE were measured for each plot at PI using a proximal and/or aerial sensor (Table 2). The proximal sensor used in this study was the GreenSeeker (GS) handheld crop sensor (Trimble Inc., Sunnyvale, CA, USA). The GS is an active sensor and measures canopy reflectance at two specific spectral wavelengths (red and near infrared) and then automatically calculates and displays the NDVI. The GS NDVI ($NDVI_{GS}$) measurements were taken while walking steadily along the edges of each plot and holding the sensor in

the nadir position at a constant height of 1.0 m above the crop canopy and extended 90 cm from the edge of the plot. For each plot, the final $NDVI_{GS}$ value represented the average of four $NDVI_{GS}$ readings. Canopy closure was achieved by PI in all plots that received N fertilizer, thus the effect of background water or soil on canopy reflectance measurements was considered negligible in those plots.

Table 2. Summary of the proximal and aerial sensors used to measure the Normalized Difference Vegetative Index (NDVI) and the Normalized Difference Red Edge (NDRE) at the panicle initiation (PI) rice growth stage.

Vegetative Index	Sensor Type	Year	Sensor	Light Source	Spectral Band	Central Wavelength (nm)	Bandwidth † (nm)	Formula	Reference
NDVI	Proximal	2017–2019	GreenSeeker	Active	Red	670	10	$\frac{(Near\ IR-Red)}{(Near\ IR+Red)}$	[48]
					Near Infrared	780	10		
	Aerial	2017	SlantRange 3P	Passive	Red	650	40		
					Near Infrared	850	100		
		2018 & 2019	MicaSense RedEdge-M	Passive	Red	668	10		
					Near Infrared	840	40		
NDRE	Aerial	2017	SlantRange 3P	Passive	Red Edge	710	20	$\frac{(Near\ IR-Red\ Edge)}{(Near\ IR+Red\ Edge)}$	[49]
					Near Infrared	850	100		
		2018 & 2019	MicaSense Red Edge-M	Passive	Red Edge	717	10		
					Near Infrared	840	40		

† full width at half maximum.

Two different aerial sensors were used in this study (Table 2). In 2017, canopy reflectance was measured using a SlantRange 3P (SlantRange Inc., San Diego, CA, USA) passive multispectral sensor. The autonomous flight mission was loaded onto the UAS using the DroneDeploy mobile app and images were captured at a height of 117 m above ground level (AGL) with 55% forward and side overlap. SlantView software (version 2.16.0) was used to process the multispectral imagery into a georeferenced orthomosaic with an average ground sampling distance of 4.8 cm $pixel^{-1}$. The SlantView software was also used to extract plot level canopy reflectance values for each of the spectral bands.

In 2018 and 2019, a MicaSense Red-Edge M (MicaSense Inc., Seattle, WA, USA) passive multispectral sensor was used to capture aerial imagery. The mobile app Pix4Dcapture was used to upload the flight mission onto the UAS, and images were captured at a height of 50 m AGL with 85% forward and side overlap. The software Pix4DMapper (version 4.2.27) was used to process the imagery into a georeferenced orthomosaic with an average ground sampling distance of 3.5 cm $pixel^{-1}$. Plot level reflectance values were extracted from the orthomosaic image using the recommended method of Haghighattalab et al. (2016) [50] as modified by Nelsen and Lundy (2021) [51].

All canopy reflectance measurements (proximal and aerial) occurred within 1 h of solar noon. In all years, the aerial sensor was mounted to a Matrice 100 UAV (DJI, Shenzhen, China). Before beginning each flight, images of a calibrated reflectance panel were taken to adjust for ambient light conditions. There was also an upwelling light sensor onboard the UAS that calibrated for incoming irradiance. Plot-level canopy reflectance values were converted into NDVI ($NDVI_{UAS}$) and NDRE ($NDRE_{UAS}$) using the formulas provided in Table 2.

2.4.2. Normalizing the Raw Vegetation Indices Using Sufficiency-Index

In order to directly compare the ability of each VI to quantify PI-N_{UP} and grain yield, the raw reflectance values from the three VIs were normalized by calculating the Sufficiency-Index (SI). The SI permits direct comparisons across VIs and measurement platforms on an equivalent numerical scale so that comparisons of statistical measures (e.g., range, slope)

are not confounded by inconsistent units among the VIs being compared. In addition, the SI produces a site-relative value such that VI values measured across multiple seasons with non-identical tools are normalized across the experiment. The SI is calculated by dividing the VI of the area of interest by the VI of an area where N was non-limiting (measured at the same location on the same day) [52]. The resulting SI values will typically range between 0 and 1, with higher values indicating a more N-sufficient crop and thus less likely to respond to additional N inputs [53–55]. In this experiment, the SI was calculated for each site by dividing the raw VI of each experimental unit by the mean VI of the experimental unit that received the highest pre-plant N application rate (using the mean VI of the highest N rate resulted in some experimental units to have a SI greater than 1.00) [56,57].

2.5. Data Analysis

Data analysis was performed using the statistical program R [58]. The degree of saturation for each index (raw VI and SI) was quantified using univariate kernel density distributions developed from the geom_density() function in the package ggplot2 [59]. For all linear regression models developed in this study, graphical and numerical summaries were examined to ensure the resulting models satisfied the assumptions of linear regression. Simple linear (quadratic) regression models were developed to quantify the relationship between pre-plant N rate and both PI-N_{UP} and grain yield at each site-year using the function lm() from the stats package [58].

Quadratic-plateau linear regression models were developed using the nls() function from the stats package [58] (following the method outlined by Mangiafico (2016) [60]) to quantify the relationships between: PI-N_{UP} and each SI; PI-N_{UP} and relative grain yield; pre-plant N rate and relative grain yield; and pre-plant N rate and each SI. For models that quantified the relationship between yield and PI-N_{UP} and N rate, the effect of site-year was initially modeled as a random effect in a mixed, nonlinear model using the nlme package [61], but convergence was not achieved. Thus, site-normalization was accomplished by expressing absolute grain yield values relative to the site-year maximum and models were fit using nls(). For each of the quadratic-plateau models, the resulting model coefficients were used to identify the mean value and associated standard error range along the x-axis where each model reached a plateau. The function nagelkerke() from the rcompanion package [62] was used to calculate a pseudo coefficient of determination (R^2) for each quadratic-plateau model [63].

Linear mixed-effects regression models were developed to quantify the sensitivity of each SI for predicting grain yield using the function lme() in the nlme package [61]. The models contained a fixed-effect for SI and random-effects of site-year slope and intercept. The response variable was grain yield. A pseudo R^2 was calculated for each mixed-effects model using the function r.squaredGLMM() in the MuMIn package [64], with the conditional R^2 representing the variability explained by the entire model (fixed and random effects), the marginal R^2 representing the variability explained only by the fixed-effects, and the portion of variability explained by the random-effects represented as the difference in conditional and marginal R^2.

3. Results

3.1. PI Total N Uptake and Grain Yield

At all sites, PI-N_{UP} was lowest in the 0N treatment and ranged from 14 (Arbuckle-18) to 75 kg N ha^{-1} (Nicolaus-17) (Figure 2, left axis). At each site, PI-N_{UP} increased with increasing pre-plant N rate. However, the magnitude of increase varied considerably across sites with maximum PI-N_{UP} ranging from 94 (Davis-19) up to 209 kg N ha^{-1} (Nicolaus-17). In most cases, PI-N_{UP} did not plateau with increasing N rate but continued to increase within the range of N rates used in this study.

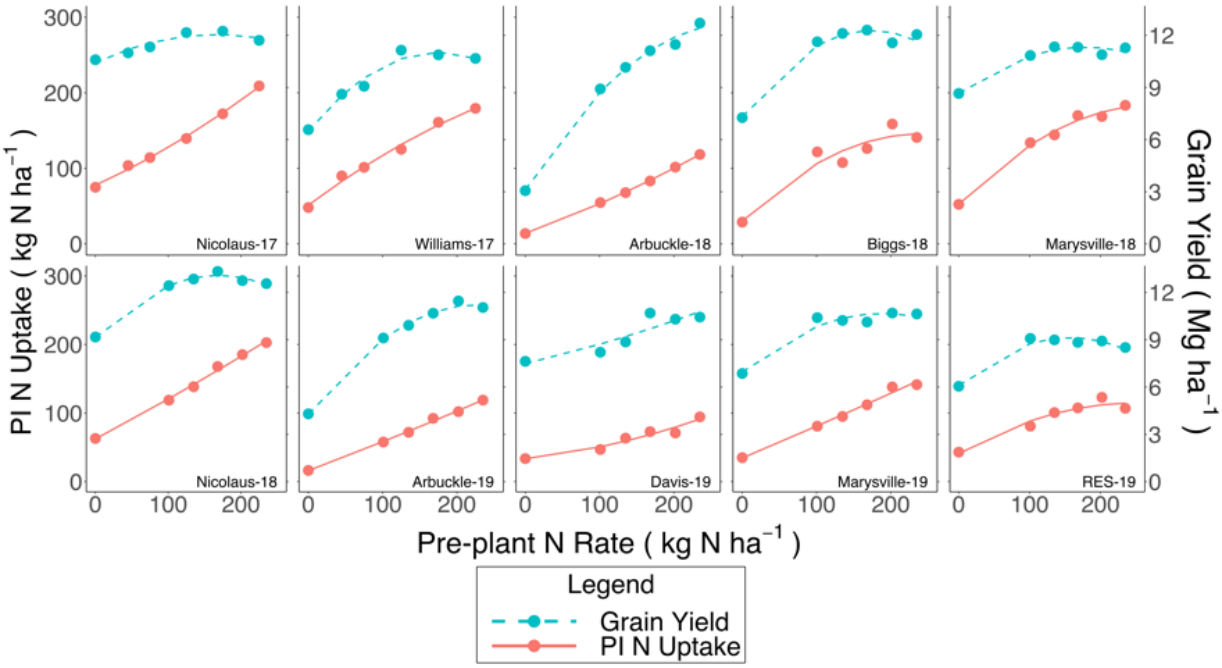

Figure 2. The relationship between pre-plant N rate and panicle initiation N uptake (PI-N_{UP}) (left axis) and grain yield (right axis) as described by quadratic linear regression models.

Similarly, at every site, grain yield was lowest in the 0N treatment, ranging from 3.1 (Arbuckle-18) up to 10.6 Mg ha^{-1} (Nicolaus-17) (Figure 2, right axis). Across all sites, yields increased with increasing pre-plant N rate up to a maximum and either plateaued or decreased at the highest N rates (with the exception of Arbuckle-18). Maximum yields ranged from 9.1 (RES-19) to 13.3 Mg ha^{-1} (Nicolaus-18). Based on the quadratic-plateau linear regression model, across sites maximum yields were achieved with an average pre-plant N rate of 183 kg N ha^{-1} (±18 kg N ha^{-1}) (Figure S1). Using a similar model, maximum yields were achieved across sites when PI-N_{UP} was ≥109 kg N ha^{-1} (±4 kg N ha^{-1}) (Figure 3).

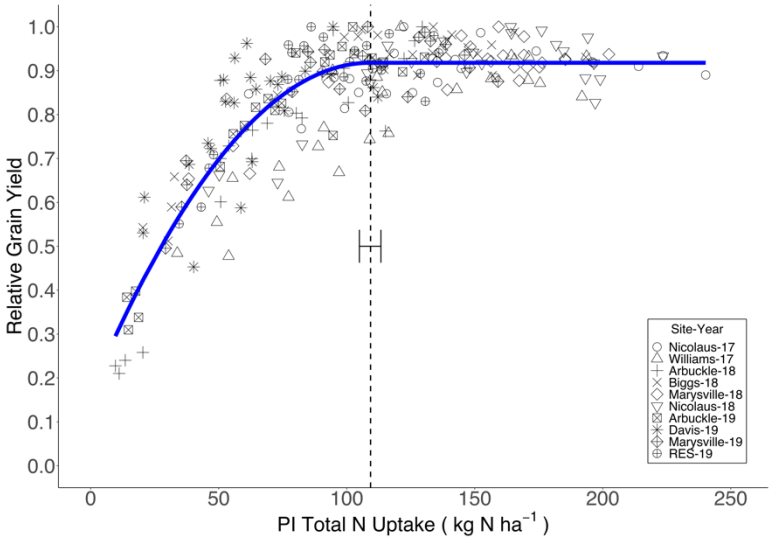

Figure 3. The relationship between total N uptake at panicle initiation rice growth stage (PI-N_{UP}) and relative grain yield as described by a quadratic-plateau linear regression model. The vertical dashed line at 109 kg N ha^{-1} represents the PI-N_{UP} value where the relationship reaches a plateau, and the error bar around the line represents the standard error.

3.2. Canopy Reflectance Data

There were differences in the kernel density distributions among the three indices in this study, both in terms of raw VI and SI (Figure 4). With respect to raw VI, $NDVI_{UAS}$ exhibited the strongest saturation, as seen by the relatively high and narrow peak of $NDVI_{UAS}$ VI observations centered around 0.90 (Figure 4a). The $NDRE_{UAS}$ exhibited the least amount of saturation as the peak of $NDRE_{UAS}$ VI values was lower and broader than the other two indices. The $NDVI_{GS}$ was more saturated than $NDRE_{UAS}$, as seen by the higher and narrower peak of $NDVI_{GS}$ VI observations. However, the $NDVI_{GS}$ did detect lower values and was thus spread over a greater range than $NDRE_{UAS}$.

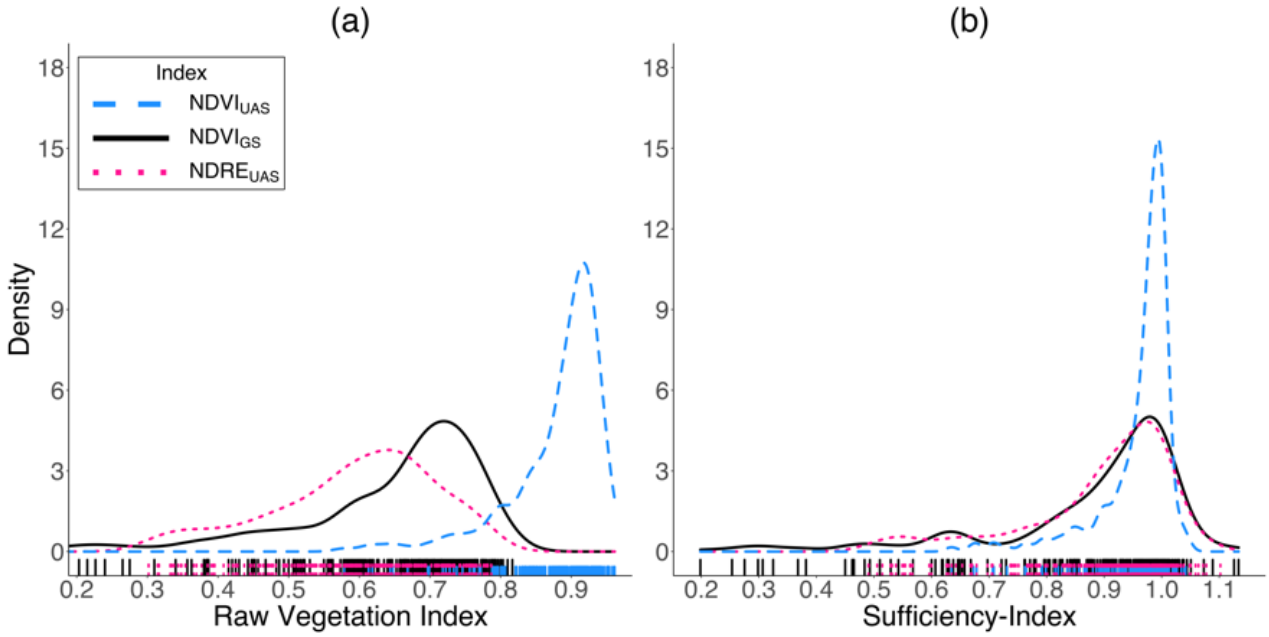

Figure 4. Kernel density distributions of unmanned aircraft system (UAS) Normalized Difference Vegetation Index ($NDVI_{UAS}$), GreenSeeker (GS) NDVI ($NDVI_{GS}$), and UAS Normalized Difference Red-Edge Index ($NDRE_{UAS}$) (**a**) raw vegetation index (VI) and (**b**) Sufficiency-Index (SI) measured at the panicle initiation (PI) rice growth stage.

Similarly, with respect to SI, the $NDVI_{UAS}$ was the most saturated with 92% of the observations being $\geq$0.85 and having the narrowest range (0.63 to 1.04) (Figure 4b). The $NDVI_{GS}$ had a larger range of SI observations (0.20 to 1.13) than $NDRE_{UAS}$ (0.49 to 1.10); but both were similarly saturated as illustrated by the proportion of $NDVI_{GS}$ (73%) and $NDRE_{UAS}$ (74%) observations that were $\geq$0.85.

3.3. Relationship between N Rate and PI-N_{UP} and Sufficiency-Index

To determine if the differences in saturation affected the ability of each index to accurately quantify the N status of the crop, quadratic-plateau linear regression models were developed to describe the relationship between PI-N_{UP} and each SI (Figure 5). In each case, SI increased with increasing PI-N_{UP} up to a threshold where it reached a plateau. The R^2 values (0.75 to 0.82) were similar for the different indices; however, the $NDVI_{UAS}$ was the least sensitive to changes in PI-N_{UP}, as it plateaued (i.e., saturated) at the lowest PI-N_{UP} (96 kg N ha^{-1}) and had the narrowest range of observations along the y-axis (0.63 to 0.99) prior to its point of saturation (Figure 5c). In contrast, the $NDVI_{GS}$ and $NDRE_{UAS}$ were more sensitive to changes in PI-N_{UP} as illustrated by saturation at higher PI-N_{UP} values (111 and 130 kg N ha^{-1}, respectively). In addition, they had broader ranges of SI observations along the y-axis (0.20 to 0.97 and 0.49 to 0.97, respectively) prior to their respective points of saturation (Figure 5a,b). Similarly, quadratic-plateau linear regression models were developed to quantify the relationship between SI and pre-plant N rate and

determine at what pre-plant N rates the different indices saturated. Each SI increased with increasing pre-plant N rate until a plateau was reached (Figure 6). The $NDVI_{UAS}$ saturated at the lowest N rate (166 ± 14 kg N ha^{-1}), followed by $NDVI_{GS}$ (207 ± 14 kg N ha^{-1}) and $NDRE_{UAS}$ (240 kg N ha^{-1} ± 15 kg N ha^{-1}).

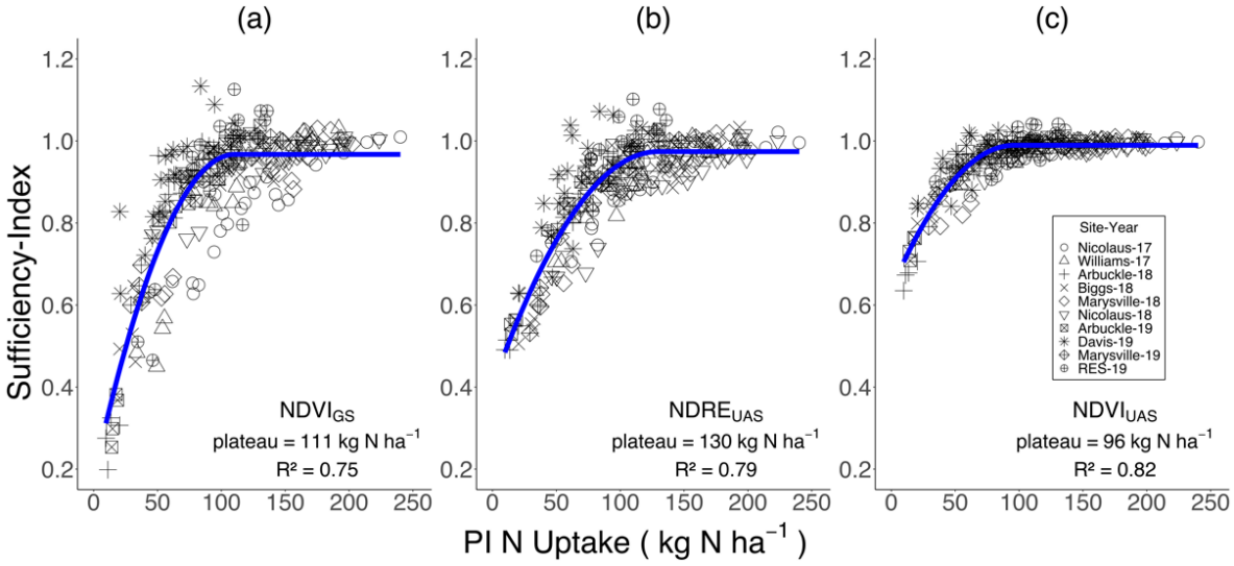

Figure 5. The relationship between panicle initiation N uptake (PI-N_{UP}) and (**a**) GreenSeeker (GS) Normalized Difference Vegetation Index ($NDVI_{GS}$) Sufficiency-Index (SI), (**b**) unmanned aircraft system (UAS) Normalized Difference Red-Edge Index ($NDRE_{UAS}$) SI, and (**c**) $NDVI_{UAS}$ SI as described by quadratic-plateau linear regression models. The plateau value reported in each panel represents the PI-N_{UP} value where the regression model reached a plateau (i.e., the point of saturation for each index).

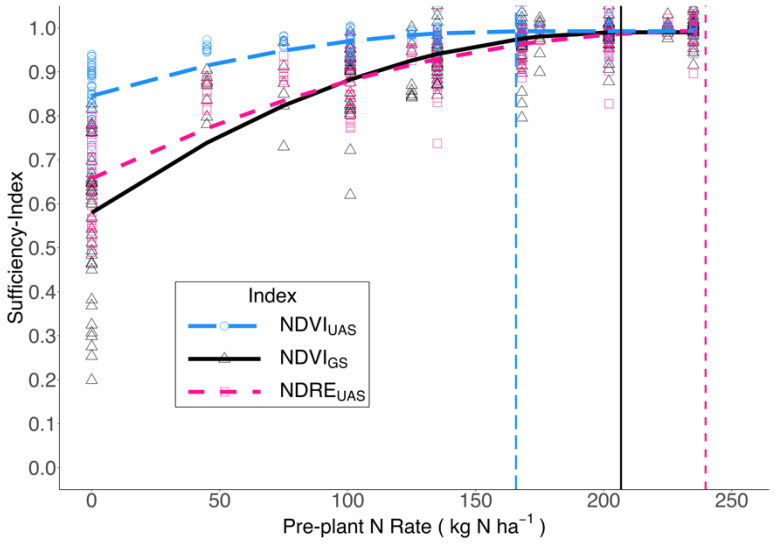

Figure 6. The relationship between pre-plant N rate and GreenSeeker (GS) Normalized Difference Vegetation Index ($NDVI_{GS}$) Sufficiency-Index (SI), unmanned aircraft system (UAS) Normalized Difference Red-Edge Index ($NDRE_{UAS}$) SI, and $NDVI_{UAS}$ SI measured at panicle initiation (PI) rice growth stage as described by quadratic-plateau linear regression models. The vertical lines represent the N rate where the relationship for each SI reaches a plateau (i.e., the point of saturation for each index).

3.4. Relationship between SI Measured at PI and Grain Yield

The sensitivity of each SI for predicting grain yield was quantified using the slope of linear mixed-effects models where yield was the response variable and SI was the

independent variable. The greater (or steeper) the slope, the less sensitive the index is in determining grain yield. The slope of $NDVI_{UAS}$ (2.4 Mg ha^{-1} per 0.1 SI) was more than double than that for $NDVI_{GS}$ (0.9 Mg ha^{-1} per 0.1 SI) and $NDRE_{UAS}$ (1.1 Mg ha^{-1} per 0.1 SI) (Figure 7). In addition, 87% of experimental units measured using $NDVI_{UAS}$ had SI $\geq$ 0.90 compared to 62% and 66% for $NDRE_{UAS}$ and $NDVI_{GS}$, respectively. With many more undifferentiated SI observations, the variability around the yield outcomes for the $NDVI_{UAS}$ observations was greater as well. Specifically, the standard deviation for site-relative grain yield was 10% for SI observations $\geq$0.90 measured via $NDVI_{UAS}$, compared to 6% and 7% for $NDRE_{UAS}$ and $NDVI_{GS}$, respectively (data not shown). This indicates that for the same experimental unit, N status at PI was measured with greater sensitivity via $NDRE_{UAS}$ and $NDVI_{GS}$ than by $NDVI_{UAS}$, and therefore yield differentiation was less variable for the former two indices than for $NDVI_{UAS}$.

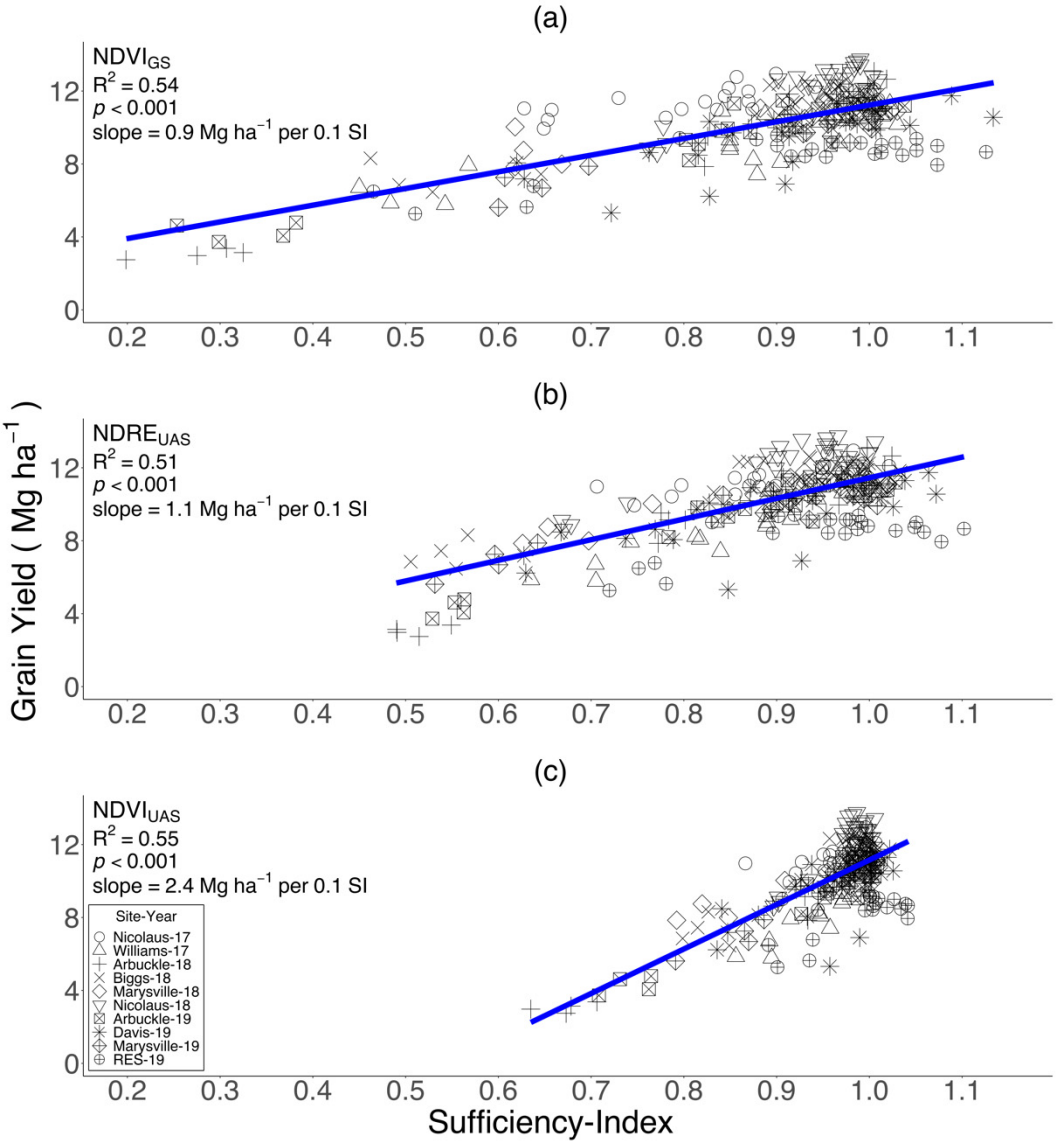

Figure 7. The relationship between (**a**) GreenSeeker Normalized Difference Vegetation Index ($NDVI_{GS}$) Sufficiency-Index (SI), (**b**) unmanned aircraft system (UAS) Normalized Difference Red-Edge Index ($NDRE_{UAS}$) SI, and (**c**) $NDVI_{UAS}$ SI measured at panicle initiation (PI) rice growth stage and grain yield as described by linear mixed-effects models. The coefficient of determination (R^2) reported in each panel represents the proportion of variability explained by the model fixed effects only.

4. Discussion

4.1. Crop Response to N Fertilizer

Maximum grain yields ranged from 10.7 Mg ha^{-1} to 13.3 Mg ha^{-1} (Figure 2), which is within 75% of the maximum yield potential for this region [65], suggesting that the sites were not limited for other nutrients besides N and were not significantly affected by diseases or pests. The RES-19 site had lower maximum yields (9.1 Mg ha^{-1}), but this may be due to planting in June, which was later than the other sites and later than the typical planting time for rice in CA [46]. Grain yield plateaued in response to pre-plant N rate at all but one site (Arbuckle-18), which confirms that the highest N rate was not N limited and thus served as a valid non-N-limiting plot to calculate the SI.

The fertilizer N rate required to achieve maximum yields across sites ranged from 165 kg N ha^{-1} up to 201 kg N ha^{-1} and averaged 183 kg N ha^{-1} (Figure S1), which is similar to the optimal N requirement reported by others for rice in CA [7,66].

Observed variability in N fertilizer response across sites in this study might be expected, given that trials were established over a 3-year period at varying locations with differing soils, management practices, and micro-climates. Similarly, there were large differences in the indigenous N supply of the soil as indicated by the wide range of PI-N_{UP} (14 to 75 kg N ha^{-1}) and yields (3.1 to 10.6 Mg ha^{-1}) in the 0N treatments across sites (Figure 2). Such variation in indigenous N supply across rice fields is common, yet it is difficult to predict and can have a large impact on optimal N fertilizer rates [67]. Across all sites, maximum PI-N_{UP} ranged from 94 kg N ha^{-1} to 209 kg N ha^{-1} (Figure 2, left axis). Unlike yields, PI-N_{UP} did not plateau at most sites, illustrating the ability of rice to take up large and even luxury amounts of N by PI as has also been shown by others [68]. The variability in indigenous N supply and N response seen in this study highlight the need to develop tools (such as canopy reflectance measurements) that can determine crop N status and help to optimize field- and year-specific N fertilizer management.

4.2. Index Saturation

Among the three indices evaluated in this study, $NDVI_{UAS}$ exhibited the greatest degree of saturation, while the $NDVI_{GS}$ and $NDRE_{UAS}$ were less saturated (Figure 4). This was seen in both the raw VI (Figure 4a) and SI (Figure 4b) data. Saturation of red-based two-band indices, such as NDVI, is a well-documented problem [17,69], and a growing body of research has reported that red-edge-based indices, such as the NDRE, are less affected by saturation and can provide a better estimation of crop N status than NDVI, especially at higher levels of crop biomass [29,30,70]. Saturation of NDVI is attributed to the crop reaching 100% canopy cover but crop biomass beneath the canopy continuing to increase [17,71]. Once the crop reaches 100% canopy cover, near infrared reflectance continues to rise, but red reflectance remains relatively constant due to strong absorption by chlorophyll at the top of the canopy, thus resulting in a minimal change in the overall ratio (i.e., the denominator will have a greater impact on the ratio than the numerator) [19,72]. Red-edge radiation can penetrate deeper into the crop canopy due to relatively lower chlorophyll absorption, causing it to be more sensitive to chlorophyll content within the entire canopy, especially at higher biomass levels [29,73]. Given this greater sensitivity to total chlorophyll content within the canopy, red-edge-based indices are able to partially overcome the saturation problem inherent to NDVI [74,75].

A difference in saturation was also observed between the two NDVI-based indices, with the $NDVI_{UAS}$ saturating more than $NDVI_{GS}$ (Figure 4). Similarly, Duan et al. (2017) [44] reported from a wheat trial that $NDVI_{UAS}$ was strongly correlated with $NDVI_{GS}$, but the $NDVI_{UAS}$ readings were offset by about 0.2 units higher and were more compressed. A likely explanation for this difference could be that compared to the $NDVI_{GS}$, which is measured using an active sensor close to the canopy, the passive multispectral sensor used to measure $NDVI_{UAS}$ cannot sample the small amount of background noise from a higher altitude due to lower spatial resolution, which results in a higher $NDVI_{UAS}$ value with a smaller range [44].

Interestingly, $NDVI_{GS}$ and $NDRE_{UAS}$ both exhibited a similar degree of saturation (Figure 4). Given the lack of comparable studies, it is difficult to be certain what may be the explanation for this result. A possible explanation could be that despite being a red-based index, the closer proximity and active light of the $NDVI_{GS}$ allows it to overcome saturation to such a degree that it exhibits a similar level of saturation as the red-edge-based $NDRE_{UAS}$. It is also worth mentioning that $NDVI_{GS}$ had a larger range of observations than $NDRE_{UAS}$. Given this, it could be argued that $NDVI_{GS}$ is a more sensitive index. However, upon closer examination, the larger range of $NDVI_{GS}$ is attributable to relatively few observations that were measured in the unfertilized N treatment at a single site. The combination of the sparse stand at that site and the smaller sampling area of the $NDVI_{GS}$ compared to $NDRE_{UAS}$ may have magnified the noise-to-signal ratio in the $NDVI_{GS}$, which led to unusually low $NDVI_{GS}$ measurements [76]. Given that all other metrics of index sensitivity are functionally equivalent or favor $NDRE_{UAS}$, this difference in range should not be over-interpreted.

4.3. Practical Implications of Index Saturation

4.3.1. Approaches for Comparing Indices

A unique aspect of this study is the quantitative approach used to assess the sensitivity of the indices. For example, each VI was normalized by calculating the SI, which allows for the comparison across the different indices on an equivalent numeric scale [57]. Moreover, the sensitivity of each index was assessed with respect to where each SI saturated and was then related to relevant thresholds for N management within this system. This approach is in contrast to most previous agronomic studies in which the utility of an index is based on raw VI values and the R^2 of the regressions [39,77,78]. If such an approach were applied to this study, $NDVI_{UAS}$ would have been identified as the best index in the two cases examined, given its higher R^2 for PI-N_{UP} (Figure 5) and yield (Figure 7). However, when the point of saturation was quantified in relationship to where information was critical to making an informed management decision (i.e., for a mid-season N status assessment), the $NDVI_{UAS}$ performed the poorest. Similarly, the approach used for yield assessment quantified the sensitivity of the index to predict grain yield based on the slope of the relationship, and again the $NDVI_{UAS}$ was the least sensitive index. Therefore, more nuanced approaches are required when comparing across indices to understand the practical value of these tools to crop management.

4.3.2. Assessing Crop N Status and Predicting Grain Yield at PI

Assessing crop N status and predicting potential grain yield early in the season is of interest to farmers and agricultural stakeholders for a number of reasons, including refining N management, planning harvest, forecasting milling and storage needs, and directing marketing strategies. Refining N management requires an understanding of crop N status and the likelihood of the crop to respond to additional N inputs. In addition, this understanding must be gained early enough in the growing season so that subsequent N management decisions can still improve yields. Panicle initiation is an optimal and important stage for assessing N status and predicting grain yield in rice for several reasons. For example, PI marks the physiological shift from plant vegetative to reproductive growth [5], N applications later than PI are less efficiently utilized to affect yield outcomes [79], and in CA rice systems, most (if not all) pre-plant N fertilizer has been taken up by this stage [80,81]. Additionally, PI is an optimal time to collect canopy reflectance data, as measurements taken much earlier than PI can often experience a strong influence of background water and soil [76], while measurements taken after PI typically saturate or are obscured by panicle emergence causing interference in the spectral signal [18,82]. Importantly, while PI may be the best time with the sensors currently available, PI occurs roughly 45 to 55 days after planting, whereas the time to harvest is usually 130 to 150 days. This leaves almost two-thirds of the growing season in which multiple factors (biological, climate, etc.) can also impact the final yields. Thus, precision of sensor-based measurements taken at PI

will be higher under circumstances in which such factors do not limit crop growth post-PI. However, across 10 site-years, SI measurements taken at PI explained over half of the total variation in absolute grain yields (Figure 7) and more than two-thirds of the variation in site-relative yields (data not shown).

In terms of making midseason N management decisions, a key question is whether or not the indices saturate at a level that renders them useful. This was evaluated using two approaches. First, it was determined that, on average, a rice crop would respond to additional N fertilizer if PI-N_{UP} was below 109 kg N ha^{-1} ($\pm$4 kg N ha^{-1}) (Figure 3). The $NDVI_{UAS}$ saturated at a PI-N_{UP} of 96 kg N ha^{-1} (Figure 5) (below 109 kg N ha^{-1}), compared to the saturation points for $NDVI_{GS}$ and $NDRE_{UAS}$ at 111 and 130 kg N ha^{-1}, respectively. These data indicate that the $NDVI_{UAS}$ is the least useful for assessing midseason crop N status as it saturates at a level of PI-N_{UP} that is less than the crop would need to ensure sufficiency and maximize yield on average. It also suggests that the $NDRE_{UAS}$ may be the most sensitive index given its relatively high saturation point with respect to PI-N_{UP}.

The second approach used to assess relative saturation of the indices and their practical value was to examine where each SI saturated based on the preseason N rate applied. The recommended N management strategy for CA rice farmers is to apply the average seasonal N requirement before flooding and planting, and then assess crop N status at PI to determine if additional fertilizer N inputs are needed [6,66]. A similar recommendation is made for direct seeded rice systems in the Mid-South USA and Australia [83–86]. In CA, typical pre-plant N rates range from 150 to 200 kg N ha^{-1}, and data from this study generally support that range with N rates required for maximum yields ranging between 165 and 201 kg N ha^{-1} (Figure S1). The average pre-plant N rate at which $NDVI_{UAS}$ saturated was 166 kg N ha^{-1}, compared to 207 and 240 kg N ha^{-1} for $NDVI_{GS}$ and $NDRE_{UAS}$ SI, respectively (Figure 6). This suggests that for the pre-plant N rates typically used in this system, the $NDRE_{UAS}$ promises the most utility as it is sensitive across a much wider range of pre-plant N rates, including those that exceed the upper limit of the recommended range. In contrast, $NDVI_{UAS}$ appears to saturate before the relevant range of measurement. Importantly, both approaches used to determine index saturation and practical utility arrive at the same conclusion.

To our knowledge, this is the first study to evaluate the comparative ability of $NDVI_{GS}$, $NDVI_{UAS}$, and $NDRE_{UAS}$ for assessing crop N status or predicting grain yield in any major cereal crop. Previous studies comparing aerial and proximal sensors generally agree with the results presented here. For example, Zheng et al. (2018) [41] reported that proximal NDVI (measured with a hyperspectral sensor) was better correlated with rice N concentration than $NDVI_{UAS}$, a finding they attributed to less saturation of the proximal NDVI. In another study, Sumner et al. (2021) [42] reported that proximal NDVI (measured with a Yara N-Sensor) and $NDRE_{UAS}$ were more sensitive to changes in N fertilizer rate than $NDVI_{UAS}$ in maize. Among studies that only used aerial sensors to assess crop N status, the results of the current study agree with the findings of Dunn et al. (2016) [28], who also found that $NDVI_{UAS}$ and $NDRE_{UAS}$ both correlate well with rice PI-N_{UP} but that $NDRE_{UAS}$ saturated less than $NDVI_{UAS}$ and provided a better basis for assessment.

In addition to the approaches mentioned above for N status assessment, the sensitivity of each index to predict grain yield at PI was quantified as the slope of the relationship between each SI and yield. The greater (or steeper) the slope, the less sensitive the index is in determining grain yield. As was the case when assessing N status, the $NDVI_{UAS}$ was also the least sensitive index for predicting yields, with SI values being confined to a narrower range of SI and thus having a higher slope (Figure 7). Both the $NDVI_{GS}$ and $NDRE_{UAS}$ were more sensitive to changes in yields and had a slope less than half of $NDVI_{UAS}$. These data indicate that $NDVI_{GS}$ and $NDRE_{UAS}$ have improved sensitivity for predicting grain yields over $NDVI_{UAS}$ at PI, which aligns with our findings regarding the relative sensitivity of each index for assessing crop N status. Although Zhou et al. (2017) [87] based their comparisons on R^2, which is different from the approach used in the current study, the conclusions of both studies are similar, as they also found that $NDRE_{UAS}$ (R^2 = 0.75) was

better for predicting rice grain yield than $NDVI_{UAS}$ (R^2 = 0.66) when compared at the booting stage (a few weeks after PI). Overall, the findings presented here can improve precision N management in this system by allowing farmers to utilize those indices that have suitable sensitivity for assessing crop N status and predicting yield at PI over those that lack the required sensitivity.

5. Conclusions

A unique approach was used to quantitatively assess the sensitivity of different VIs on a common numeric scale. Results indicated that both the $NDRE_{UAS}$ and $NDVI_{GS}$ measured rice crop N status and grain yield at PI with similar sensitivity. This is despite the fact that the former was measured using an aerial sensor at least 50 m above the crop while the latter was measured using an active proximal sensor within 1 m of the crop canopy. The ability to assess crop status effectively across different sensors provides a unique advantage for end-users as it allows flexibility to choose the sensor most suitable for their goals. In contrast, the $NDVI_{UAS}$ had much less utility for the purposes examined in this paper. These findings should improve fertilizer management in these systems by identifying indices that serve as a better basis for the development of precision N management strategies. Given the relatively small number of studies that have explored this topic, additional studies are required to better understand how these results may be affected by the choice of rice variety, growth stage, biophysical parameter, or crop. Furthermore, with the rapid development of new sensors (both aerial and spaceborne) with higher spatial and spectral resolution, future research in this area should also explore how the findings presented here may be affected by the use of different platforms, sensors, or VIs.

Supplementary Materials: The following supporting information can be downloaded at: https://www.mdpi.com/article/10.3390/rs14122770/s1, Figure S1. The relationship between pre-plant N rate and relative rice grain yield as described by a quadratic-plateau linear regression model. The vertical dashed line at 183 kg N ha^{-1} represents the N rate where the relationship reaches a plateau, and the error bar around the line represents the standard error.

Author Contributions: Conceptualization, B.A.L.; methodology, B.A.L., T.H.R. and M.E.L.; software, T.H.R. and M.E.L.; formal analysis, T.H.R. and M.E.L.; investigation, T.H.R.; resources, B.A.L.; data curation, T.H.R.; writing—original draft preparation, T.H.R.; writing—review and editing, B.A.L. and M.E.L.; visualization, T.H.R.; supervision, B.A.L.; project administration, T.H.R. and B.A.L.; funding acquisition, B.A.L. All authors have read and agreed to the published version of the manuscript.

Funding: This research was funded by The California Rice Research Board, grant number RR19-7.

Data Availability Statement: The data and R script used to perform the analysis and generate this manuscript are openly available on GitHub and archived in Zenodo at https://doi.org/10.5281/zenodo.6621415 (accessed on 5 May 2022).

Acknowledgments: The authors would like to thank Cesar Abrenilla and fellow members of the Agroecosystems Lab, Ray Stogsdill and the entire staff at the California Rice Experiment Station, visiting scholars Muhammad Ishfaq, Wencheng Ding, and Kevin Cassman for their assistance in the field and laboratory, and the California rice farmers who participated in this study.

Conflicts of Interest: The authors declare no conflict of interest.

References

1. Hatfield, J.L.; Gitelson, A.A.; Schepers, J.S.; Walthall, C.L. Application of Spectral Remote Sensing for Agronomic Decisions. *Agron. J.* **2008**, *100*, 117–131. [CrossRef]
2. Xue, J.; Su, B. Significant Remote Sensing Vegetation Indices: A Review of Developments and Applications. *J. Sens.* **2017**, *2017*, 1353691. [CrossRef]
3. Hatfield, J.L.; Prueger, J.H.; Sauer, T.J.; Dold, C.; O'Brien, P.; Wacha, K. Applications of Vegetative Indices from Remote Sensing to Agriculture: Past and Future. *Inventions* **2019**, *4*, 71. [CrossRef]
4. Toth, C.; Jóźków, G. Remote Sensing Platforms and Sensors: A Survey. *ISPRS J. Photogramm.* **2016**, *115*, 22–36. [CrossRef]
5. De Datta, S.K. *Principles and Practices of Rice Production*; International Rice Research Institute: Los Baños, Philippines, 1981.

6. Williams, J.F. *Rice Nutrient Management in California*; University of California Agriculture and Natural Resources Publication: Davis, CA, USA, 2010; Volume 3516.
7. Tamagno, S.; Eagle, A.J.; McLellan, E.L.; van Kessel, C.; Linquist, B.A.; Ladha, J.K.; Pittelkow, C.M. Quantifying N Leaching Losses as a Function of N Balance: A Path to Sustainable Food Supply Chains. *Agric. Ecosyst. Environ.* **2022**, *324*, 107714. [CrossRef]
8. Pittelkow, C.M.; Adviento-Borbe, M.A.; van Kessel, C.; Hill, J.E.; Linquist, B.A. Optimizing rice yields while minimizing yield-scaled global warming potential. *Global Change Biol.* **2014**, *20*, 1382–1393. [CrossRef]
9. Smith, J.; Sutula, M.; Bouma-Gregson, K.; Van Dyke, M. *California Water Boards' Framework and Strategy for Freshwater Harmful Algal Bloom Monitoring: Executive Synthesis*; Southern California Coastal Water Research Project Technical Report for California State Water Resources Control Board: Sacramento, CA, USA, 2021; pp. 1141.A:1–1141.A:220.
10. Daughtry, C.S.T.; Walthall, C.L.; Kim, M.S.; Brown de Colstoun, E.; McMurtrey, J.E., III. Estimating Corn Leaf Chlorophyll Concentration from Leaf and Canopy Reflectance. *Remote Sens. Environ.* **2000**, *74*, 229–239. [CrossRef]
11. Balasubramanian, V.; Morales, A.C.; Cruz, R.T.; Abdulrachman, S. On-Farm Adaptation of Knowledge-Intensive Nitrogen Management Technologies for Rice Systems. *Nutr. Cycl. Agroecosys.* **1999**, *53*, 59–69. [CrossRef]
12. Witt, C.; Pasuquin, J.M.C.A.; Mutters, R.; Buresh, R.J. New Leaf Color Chart for Effective Nitrogen Management in Rice. *Better Crop.* **2005**, *89*, 36–39.
13. Saberioon, M.M.; Amin, M.S.M.; Gholizadeh, A.; Ezri, M.H. A Review of Optical Methods for Assessing Nitrogen Contents during Rice Growth. *Appl. Eng. Agric.* **2014**, *30*, 657–669. [CrossRef]
14. Colomina, I.; Molina, P. Unmanned Aerial Systems for Photogrammetry and Remote Sensing: A Review. *ISPRS J. Photogramm.* **2014**, *92*, 79–97. [CrossRef]
15. Mulla, D.J. Twenty Five Years of Remote Sensing in Precision Agriculture: Key Advances and Remaining Knowledge Gaps. *Biosyst. Eng.* **2013**, *114*, 358–371. [CrossRef]
16. Tucker, C.J. Red and Photographic Infrared Linear Combinations for Monitoring Vegetation. *Remote Sens. Environ.* **1979**, *8*, 127–150. [CrossRef]
17. Huang, S.; Tang, L.; Hupy, J.P.; Wang, Y.; Shao, G. A Commentary Review on the Use of Normalized Difference Vegetation Index (NDVI) in the Era of Popular Remote Sensing. *J. For. Res.* **2021**, *32*, 1–6. [CrossRef]
18. Harrell, D.L.; Tubana, B.S.; Walker, T.W.; Phillips, S.B. Estimating Rice Grain Yield Potential Using Normalized Difference Vegetation Index. *Agron. J.* **2011**, *103*, 1717–1723. [CrossRef]
19. Rehman, T.R.; Reis, A.F.B.; Akbar, N.; Linquist, B.A. Use of Normalized Difference Vegetation Index to Assess N Status and Predict Grain Yield in Rice. *Agron. J.* **2019**, *111*, 2889–2898. [CrossRef]
20. Yao, Y.; Miao, Y.; Huang, S.; Gao, L.; Ma, X.; Zha, G.; Jiang, R.; Chen, X.; Zhang, F.; Yu, K.; et al. Active Canopy Sensor-Based Precision N Management Strategy for Rice. *Agron. Sustain. Dev.* **2012**, *32*, 925–933. [CrossRef]
21. Li, Y.; Chen, D.; Walker, C.N.; Angus, J.F. Estimating the Nitrogen Status of Crops Using a Digital Camera. *Field Crop. Res.* **2010**, *118*, 221–227. [CrossRef]
22. Teal, R.K.; Tubana, B.; Girma, K.; Freeman, K.W.; Arnall, D.B.; Walsh, O.; Raun, W.R. In-Season Prediction of Corn Grain Yield Potential Using Normalized Difference Vegetation Index. *Agron. J.* **2006**, *98*, 1488–1494. [CrossRef]
23. Xia, T.; Miao, Y.; Wu, D.; Shao, H.; Khosla, R.; Mi, G. Active Optical Sensing of Spring Maize for In-Season Diagnosis of Nitrogen Status Based on Nitrogen Nutrition Index. *Remote Sens.* **2016**, *8*, 605. [CrossRef]
24. Tsouros, D.C.; Bibi, S.; Sarigiannidis, P.G. A Review on UAV-Based Applications for Precision Agriculture. *Information* **2019**, *10*, 349. [CrossRef]
25. Delavarpour, N.; Koparan, C.; Nowatzki, J.; Bajwa, S.; Sun, X. A Technical Study on UAV Characteristics for Precision Agriculture Applications and Associated Practical Challenges. *Remote Sens.* **2021**, *13*, 1204. [CrossRef]
26. Fu, Y.; Yang, G.; Song, X.; Li, Z.; Xu, X.; Feng, H.; Zhao, C. Improved Estimation of Winter Wheat Aboveground Biomass using Multiscale Textures Extracted from UAV-Based Digital Images and Hyperspectral Feature Analysis. *Remote Sens.* **2021**, *13*, 581. [CrossRef]
27. Esposito, M.; Crimaldi, M.; Cirillo, V.; Sarghini, F.; Maggio, A. Drone and Sensor Technology for Sustainable Weed Management: A Review. *Chem. Biol. Technol. Agric.* **2021**, *8*, 1–11. [CrossRef]
28. Dunn, B.W.; Dunn, T.S.; Hume, I.; Orchard, B.A.; Dehaan, R.; Robson, A. Remote Sensing PI Nitrogen Uptake in Rice. *IREC Newsl.* **2016**, *195*, 48–50.
29. Li, F.; Miao, Y.; Feng, G.; Yuan, F.; Yue, S.; Gao, X.; Liu, Y.; Liu, B.; Ustin, S.L.; Chen, X. Improving Estimation of Summer Maize Nitrogen Status with Red Edge-Based Spectral Vegetation Indices. *Field Crop. Res.* **2014**, *157*, 111–123. [CrossRef]
30. Dunn, B.W.; Dehaan, R.; Schmidtke, L.M.; Dunn, T.S.; Meder, R. Using Field-Derived Hyperspectral Reflectance Measurement to Identify the Essential Wavelengths for Predicting Nitrogen Uptake of Rice at Panicle Initiation. *J. Near Infrared Spec.* **2016**, *24*, 473–483. [CrossRef]
31. Small, C.; Milesi, C. Multi-Scale Standardized Spectral Mixture Models. *Remote Sens. Environ.* **2013**, *136*, 442–454. [CrossRef]
32. He, D.C.; Wang, L. Texture Unit, Texture Spectrum, and Texture Analysis. *IEEE Trans. Geosci. Remote Sens.* **1990**, *28*, 509–512.
33. Maxwell, A.E.; Warner, T.A.; Fang, F. Implementation of Machine-Learning Classification in Remote Sensing: An Applied Review. *Int. J. Remote Sens.* **2018**, *39*, 2784–2817. [CrossRef]
34. Wang, L.; Chen, S.; Li, D.; Wang, C.; Jiang, H.; Zheng, Q.; Peng, Z. Estimation of Paddy Rice Nitrogen Content and Accumulation both at Leaf and Plant Levels from UAV Hyperspectral Imagery. *Remote Sens.* **2021**, *13*, 2956. [CrossRef]

35. Zha, H.; Miao, Y.; Wang, T.; Li, Y.; Zhang, J.; Sun, W.; Feng, Z.; Kusnierek, K. Improving Unmanned Aerial Vehicle Remote Sensing-Based Rice Nitrogen Nutrition Index Prediction with Machine Learning. *Remote Sens.* **2020**, *12*, 215. [CrossRef]
36. Hardin, P.J.; Jensen, R.R. Small-Scale Unmanned Aerial Vehicles in Environmental Remote Sensing: Challenges and Opportunities. *GISci. Remote Sens.* **2011**, *48*, 99–111. [CrossRef]
37. Zhang, C.; Kovacs, J.M. The Application of Small Unmanned Aerial Systems for Precision Agriculture: A Review. *Precis. Agric.* **2012**, *13*, 693–712. [CrossRef]
38. Zheng, H.; Cheng, T.; Zhou, M.; Li, D.; Yao, X.; Tian, Y.; Cao, W.; Zhu, Y. Improved Estimation of Rice Aboveground Biomass Combining Textural and Spectral Analysis of UAV Imagery. *Precis. Agric.* **2019**, *20*, 611–629. [CrossRef]
39. Walsh, O.S.; Shafian, S.; Marshall, J.M.; Jackson, C.; McClintick-Chess, J.R.; Blanscet, S.M.; Swoboda, K.; Thompson, C.; Belmont, K.M.; Walsh, W.L. Assessment of UAV Based Vegetation Indices for Nitrogen Concentration Estimation in Spring Wheat. *Adv. Remote Sens.* **2018**, *7*, 71–90. [CrossRef]
40. Becker, T.; Nelsen, T.S.; Leinfelder-Miles, M.; Lundy, M.E. Differentiating Between Nitrogen and Water Deficiency in Irrigated Maize Using a UAV-Based Multi-Spectral Camera. *Agronomy* **2020**, *10*, 1671. [CrossRef]
41. Zheng, H.; Cheng, T.; Li, D.; Yao, X.; Tian, Y.; Cao, W.; Zhu, Y. Combining Unmanned Aerial Vehicle (UAV)-Based Multispectral Imagery and Ground-Based Hyperspectral Data for Plant Nitrogen Concentration Estimation in Rice. *Front. Plant Sci.* **2018**, *9*, 936. [CrossRef]
42. Sumner, Z.; Varco, J.J.; Dhillon, J.S.; Fox, A.A.; Czarnecki, J.; Henry, W.B. Ground Versus Aerial Canopy Reflectance of Corn: Red-Edge and Non-Red Edge Vegetation Indices. *Agron. J.* **2021**, *113*, 2782–2797. [CrossRef]
43. Hassan, M.A.; Yang, M.; Rasheed, A.; Yang, G.; Reynolds, M.; Xia, X.; Xiao, Y.; He, Z. A Rapid Monitoring of NDVI across the Wheat Growth Cycle for Grain Yield Prediction Using a Multi-Spectral UAV Platform. *Plant Sci.* **2019**, *282*, 95–103. [CrossRef]
44. Duan, T.; Chapman, S.C.; Guo, Y.; Zheng, B. Dynamic Monitoring of NDVI in Wheat Agronomy and Breeding Trials Using an Unmanned Aerial Vehicle. *Field Crop. Res.* **2017**, *210*, 71–80. [CrossRef]
45. CIMIS. California Irrigation Management Information System. *Internet Resource*. 2020. Available online: http://www.cimis.water.ca.gov/WSNReportCriteria.aspx) (accessed on 1 September 2020).
46. Hill, J.E.; Williams, J.F.; Mutters, R.G.; Greer, C.A. The California Rice Cropping System: Agronomic Resource Issues for Long-Term Sustainability. *Paddy Water Environ.* **2006**, *4*, 13–19. [CrossRef]
47. Sharp, Z. *Principles of Stable Isotope Geochemistry*, 2nd ed.; University of New Mexico Press: Albuquerque, NM, USA, 2017.
48. Rouse, J.W., Jr.; Haas, R.H.; Schell, J.A.; Deering, D.W. Monitoring Vegetation Systems in the Great Plains with ERTS. In Proceedings of the Third Earth Resources Technology Satellite-1 Symposium: Section AB. Technical Presentations, Washington, DC, USA, 10–14 December 1973.
49. Gitelson, A.A.; Merzlyak, M.N. Quantitative Estimation of Chlorophyll-A Using Reflectance Spectra: Experiments with Autumn Chestnut and Maple Leaves. *J. Photochem. Photobiol.* **1994**, *22*, 247–252. [CrossRef]
50. Haghighattalab, A.; Pérez, L.G.; Mondal, S.; Singh, D.; Schinstock, D.; Rutkoski, J.; Ortiz-Monasterio, I.; Singh, R.P.; Goodin, D.; Poland, J. Application of Unmanned Aerial Systems for High Throughput Phenotyping of Large Wheat Breeding Nurseries. *Plant Methods* **2016**, *12*, 1–15. [CrossRef]
51. Nelsen, T.; Lundy, M.; Drone Data in Agricultural Research. GitHub Repository. 2021. Available online: https://github.com/Grain-Cropping-Systems-Lab/Drone-Data-in-Agricultural-Research (accessed on 1 August 2019).
52. Colaço, A.F.; Bramley, R.G. Do Crop Sensors Promote Improved Nitrogen Management in Grain Crops? *Field Crop. Res.* **2018**, *218*, 126–140. [CrossRef]
53. Bijay-Singh; Ali, A.M. Using Hand-Held Chlorophyll Meters and Canopy Reflectance Sensors for Fertilizer Nitrogen Management in Cereals in Small Farms in Developing Countries. *Sensors* **2020**, *20*, 1127. [CrossRef]
54. Holland, K.H.; Schepers, J.S. Derivation of a Variable Rate Nitrogen Application Model for In-Season Fertilization of Corn. *Agron. J.* **2010**, *102*, 1415–1424. [CrossRef]
55. Nelsen, T.S.; Lundy, M.E. Canopy Reflectance Informs In-Season Malting Barley Nitrogen Management: An Ex-Ante Classification Approach. *Agron. J.* **2020**, *112*, 4705–4722. [CrossRef]
56. Lu, J.; Miao, Y.; Shi, W.; Li, J.; Yuan, F. Evaluating Different Approaches to Non-Destructive Nitrogen Status Diagnosis of Rice Using Portable Rapidscan Active Canopy Sensor. *Sci. Rep.* **2017**, *7*, 1–10. [CrossRef]
57. Chen, Z.; Miao, Y.; Lu, J.; Zhou, L.; Li, Y.; Zhang, H.; Lou, W.; Zhang, Z.; Kusnierek, K.; Liu, C. In-Season Diagnosis of Winter Wheat Nitrogen Status in Smallholder Farmer Fields Across a Village Using Unmanned Aerial Vehicle-Based Remote Sensing. *Agronomy* **2019**, *9*, 619. [CrossRef]
58. R Core Team. *R: A Language and Environment for Statistical Computing*; R Foundation for Statistical Computing: Vienna, Austria, 2021. Available online: https://www.R-project.org/ (accessed on 1 October 2016).
59. Wickham, H. *ggplot2: Elegant Graphics for Data Analysis*; Springer: New York, NY, USA, 2016. Available online: https://ggplot2.tidyverse.org (accessed on 1 October 2016).
60. Mangiafico, S.S. Summary and Analysis of Extension Program Evaluation in R. 2016. Available online: https://rcompanion.org/handbook (accessed on 1 April 2022).
61. Pinheiro, J.; Bates, D.; DebRoy, S.; Sarkar, D.; R Core Team. nlme: Linear and Nonlinear Mixed Effects Models. 2021. Available online: https://CRAN.R-project.org/package=nlme (accessed on 15 December 2017).
62. Mangiafico, S.S. rcompanion: Functions to Support Extension Education Program Evaluation. *Cran Repos.* **2022**, *20*, 1–71.

63. Cox, D.R.; Snell, E.J. *Analysis of Binary Data*; Chapman & Hall: Boca Raton, FL, USA, 2018.
64. Bartoń, K. MuMIn: Multi-Model Inference. 2020. Available online: https://CRAN.R-project.org/package=MuMIn (accessed on 1 August 2020).
65. Espe, M.B.; Yang, H.; Cassman, K.G.; Guilpart, N.; Sharifi, H.; Linquist, B.A. Estimating Yield Potential in Temperate High-Yielding, Direct-Seeded US Rice Production Systems. *Field Crop. Res.* **2016**, *193*, 123–132. [CrossRef]
66. Linquist, B.A.; Hill, J.E.; Mutters, R.G.; Greer, C.A.; Hartley, C.; Ruark, M.; van Kessel, C. Assessing the Necessity of Surface Applied Preplant Nitrogen Fertilizer in Rice Systems. *Agron. J.* **2009**, *101*, 906–915. [CrossRef]
67. Cassman, K.G.; Gines, G.C.; Dizon, M.A.; Samson, M.I.; Alcantara, J.M. Nitrogen-Use Efficiency in Tropical Lowland Rice Systems: Contributions from Indigenous and Applied Nitrogen. *Field Crop. Res.* **1996**, *47*, 1–12. [CrossRef]
68. Peng, S.; Cassman, K.G. Upper Thresholds of Nitrogen Uptake Rates and Associated Nitrogen Fertilizer Efficiencies in Irrigated Rice. *Agron. J.* **1998**, *90*, 178–185. [CrossRef]
69. Hatfield, J.L.; Prueger, J.H. Value of Using Different Vegetative Indices to Quantify Agricultural Crop Characteristics at Different Growth Stages Under Varying Management Practices. *Remote Sens.* **2010**, *2*, 562. [CrossRef]
70. Amaral, L.R.; Molin, J.P.; Schepers, J.S. Algorithm for Variable-Rate Nitrogen Application in Sugarcane Based on Active Crop Canopy Sensor. *Agron. J.* **2015**, *107*, 1513–1523. [CrossRef]
71. Gitelson, A.A. Wide Dynamic Range Vegetation Index for Remote Quantification of Biophysical Characteristics of Vegetation. *J. Plant Physiol.* **2004**, *161*, 165–173. [CrossRef] [PubMed]
72. Thenkabail, P.S.; Smith, R.B.; De Pauw, E. Hyperspectral Vegetation Indices and Their Relationships with Agricultural Crop Characteristics. *Remote Sens. Environ.* **2000**, *71*, 158–182. [CrossRef]
73. Miller, J.J.; Schepers, J.S.; Shapiro, C.A.; Arneson, N.J.; Eskridge, K.M.; Oliveira, M.C.; Giesler, L.J. Characterizing Soybean Vigor and Productivity Using Multiple Crop Canopy Sensor Readings. *Field Crop. Res.* **2018**, *216*, 22–31. [CrossRef]
74. Van Niel, T.G.; McVicar, T.R. Determining Temporal Windows for Crop Discrimination with Remote Sensing: A Case Study in South-Eastern Australia. *Comput. Electron. Agric.* **2004**, *45*, 91–108. [CrossRef]
75. Nguy-Robertson, A.; Gitelson, A.; Peng, Y.; Viña, A.; Arkebauer, T.; Rundquist, D. 2012. Green Leaf Area Index Estimation in Maize and Soybean: Combining Vegetation Indices to Achieve Maximal Sensitivity. *Agron. J.* **2012**, *104*, 1336–1347. [CrossRef]
76. Kanke, Y.; Tubana, B.; Dalen, M.; Harrell, D. Evaluation of Red and Red-Edge Reflectance-Based Vegetation Indices for Rice Biomass and Grain Yield Prediction Models in Paddy Fields. *Precis. Agric.* **2016**, *17*, 507–530. [CrossRef]
77. Cao, Q.; Miao, Y.; Wang, H.; Huang, S.; Cheng, S.; Khosla, R.; Jiang, R. Non-Destructive Estimation of Rice Plant Nitrogen Status with Crop Circle Multispectral Active Canopy Sensor. *Field Crop. Res.* **2013**, *154*, 133–144. [CrossRef]
78. Gnyp, M.L.; Miao, Y.; Yuan, F.; Ustin, S.L.; Yu, K.; Yao, Y.; Huang, S.; Bareth, G. 2014. Hyperspectral Canopy Sensing of Paddy Rice Aboveground Biomass at Different Growth Stages. *Field Crop. Res.* **2014**, *155*, 42–55. [CrossRef]
79. Linquist, B.A.; Sengxua, P. Efficient and Flexible Management of Nitrogen for Rainfed Lowland Rice. *Nutr. Cycl. Agroecosys.* **2003**, *67*, 139–146. [CrossRef]
80. LaHue, G.T.; Chaney, R.L.; Adviento-Borbe, M.A.; Linquist, B.A. Alternate Wetting and Drying in High Yielding Direct-Seeded Rice Systems Accomplishes Multiple Environmental and Agronomic Objectives. *Agric. Ecosyst. Environ.* **2016**, *229*, 30–39. [CrossRef]
81. Perry, H.; Carrijo, D.; Linquist, B. Single Midseason Drainage Events Decrease Global Warming Potential Without Sacrificing Grain Yield in Flooded Rice Systems. *Field Crop. Res.* **2022**, *276*, 1–13. [CrossRef]
82. Kaur, R. Prediction of Grain Yield and Nitrogen Uptake by Basmati Rice through In-Season Proximal Sensing with a Canopy Reflectance Sensor. *Precis. Agric.* **2021**, *23*, 733–747. [CrossRef]
83. Dunn, B.W.; Dunn, T.S.; Beecher, H.G. Nitrogen Timing and Rate Effects on Growth and Grain Yield of Delayed Permanent-Water Rice in South-Eastern Australia. *Crop Pasture Sci.* **2014**, *65*, 878–887. [CrossRef]
84. Dunn, B.W.; Dunn, T.S.; Orchard, B.A. Nitrogen Rate and Timing Effects on Growth and Yield of Drill-Sown Rice. *Crop Pasture Sci.* **2016**, *67*, 1149–1157. [CrossRef]
85. Norman, R.J.; Slaton, N.A.; Roberts, T.L. Soil Fertility. In *Rice Production Handbook*; Miscellaneous Publication 192, Hardke, J., Eds.; Arkansas Cooperative Extension Service: Little Rock, AR, USA, 2021; pp. 69–101.
86. Troldahl, D. *Rice Growing Guide*; New South Wales Government Department of Primary Industries: Orange, NSW, Australia, 2018; pp. 16–19.
87. Zhou, X.; Zheng, H.B.; Xu, X.Q.; He, J.Y.; Ge, X.K.; Yao, X.; Cheng, T.; Zhu, Y.; Cao, W.X.; Tian, Y.C. Predicting Grain Yield in Rice Using Multi-Temporal Vegetation Indices from UAV-Based Multispectral and Digital Imagery. *ISPRS J. Photogramm.* **2017**, *130*, 246–255. [CrossRef]